
Surface Brightness Fluctuations as Primary and Secondary Distance Indicators

John P. Blakeslee¹

Abstract The surface brightness fluctuations (SBF) method measures the variance in a galaxy’s light distribution arising from fluctuations in the numbers and luminosities of individual stars per resolution element. Once calibrated for stellar population effects, SBF measurements with *HST* provide distances to early-type galaxies with unrivaled precision. Optical SBF data from *HST* for the Virgo and Fornax clusters give the relative distances of these nearby fiducial clusters with 2% precision and constrain their internal structures. Observations in hand will allow us to tie the Coma cluster, the standard of comparison for distant cluster studies, into the same precise relative distance scale. The SBF method can be calibrated in an absolute sense either empirically from Cepheids or theoretically from stellar population models. The agreement between the model and empirical zero points has improved dramatically, providing an independent confirmation of the Cepheid distance scale. SBF is still brighter in the near-IR, and an ongoing program to calibrate the method for the F110W and F160W passbands of the Wide Field Camera 3 IR channel will enable accurate distance derivation whenever a large early-type galaxy or bulge is observed in these passbands at distances reaching well out into the Hubble flow.

1 Background

The surface brightness fluctuations (SBF) method remains one of the most accurate ways of measuring galaxy distances. Tonry & Schneider (1988) presented the original implementation of the method;

further developments were described by Tonry et al. (1990), Jensen et al. (1998), Blakeslee et al. (1999), and Mei et al. (2005a). The method determines the intrinsic variance in a galaxy image resulting from stochastic variations in the numbers and luminosities of the stars falling within individual pixels of the image. These variations in pixel intensity are blurred by the point spread function (PSF); thus, the variance measurement is done in Fourier space on the scale of the PSF, and all sources of contamination (unresolved background or foreground sources) must be taken into account. The measured variance is normalized by the local galaxy surface brightness and then converted to the apparent SBF magnitude \overline{m} . If the galaxy distance is known, then the absolute SBF magnitude \overline{M} provides useful information on the properties of the most luminous stars within the galaxy, and measurements of \overline{m} in different bandpasses yield “fluctuation colors” that provide distance-independent constraints on the stellar population. For more about using SBF for stellar population studies, see recent works by Cantiello et al. (2007b), Raimondo (2009), Blakeslee (2009), González-Lópezlira et al. (2010), and Lee et al. (2010).

For the purpose of estimating galaxy distances, the absolute \overline{M} must be predicted accurately from stellar population synthesis models (SBF as a primary distance indicator) or from an empirical calibration (secondary distance indicator). The distance modulus, $\overline{m} - \overline{M}$ then follows directly. As the SBF method has been around for over two decades, the estimated distances have been compared to those produced by many other methods, including Cepheids (Tonry et al. 1997, 2000; Ferrarese et al. 2000), Type Ia supernovae (Ajhar et al. 2001), the fundamental plane (Blakeslee et al. 2002), the planetary nebula luminosity function (Ciardullo et al. 2002), and the tip of the red giant branch (Mould & Sakai 2009). However, in most

John P. Blakeslee

Dominion Astrophysical Observatory, Herzberg Institute of Astrophysics, National Research Council of Canada, Victoria, BC V9E 2E7, Canada

cases, these comparisons involve the ground-based SBF distances from Tonry et al. (2001). Blakeslee et al. (2009, 2010) compare the recent SBF results from the *Hubble Space Telescope* (*HST*) to earlier ground-based work and discuss the reliability and limits of the older data (see in particular Appendix A of Blakeslee et al. 2010), as well as zero-point calibration issues. The purpose of the present contribution is to describe the current state of the SBF art and foreshadow future developments. The treatment here is woefully incomplete, and the interested reader should consult the original works for further details.

2 SBF Studies with *HST*/ACS

Most of the recent observational work on SBF distances has been carried out with the Advanced Camera for Surveys (ACS) on board *HST*. Earlier *HST* studies using WFPC2 were limited by the sensitivity, field size, and/or sampling of that instrument. The installation of ACS on *HST* made the SBF method far more powerful. The ACS Wide Field Channel (ACS/WFC) samples the PSF with a resolution comparable to WFPC2’s planetary camera detector ($40''$ field), but over a much larger $\sim 3'3$ field of view and with about five times the throughput at the red wavelengths typically used for SBF distance measurements. These characteristics made it possible to measure significant radial gradients in the SBF amplitude, corresponding to stellar population gradients, for sizable samples of early-type galaxies (Cantiello et al. 2005, 2007b). ACS also vastly improved the precision of mean SBF magnitudes, and thus of galaxy distances.

2.1 ACS Virgo Cluster Survey

The ACS Virgo Cluster Survey (ACSVCS, Côté et al. 2004) is a Large Program with *HST* targeting 100 early-type galaxies in the Virgo cluster with the F475W (g_{475}) and F850LP (z_{850}) bandpasses. The goals of the survey include detailed, high-resolution studies of galaxy nuclei and central structure, the properties of thousands of globular clusters in the program galaxies, and the structure of the Virgo cluster as determined by SBF distance measurements. Here, we concentrate on the distance results.

This survey posed a number of challenges for the SBF method. The off-axis ACS instrument has significant spatial distortion, and the standard linear interpolation kernel used for the image rectification had severe implications for the image power spectrum, making the usual SBF analysis impossible. As discussed

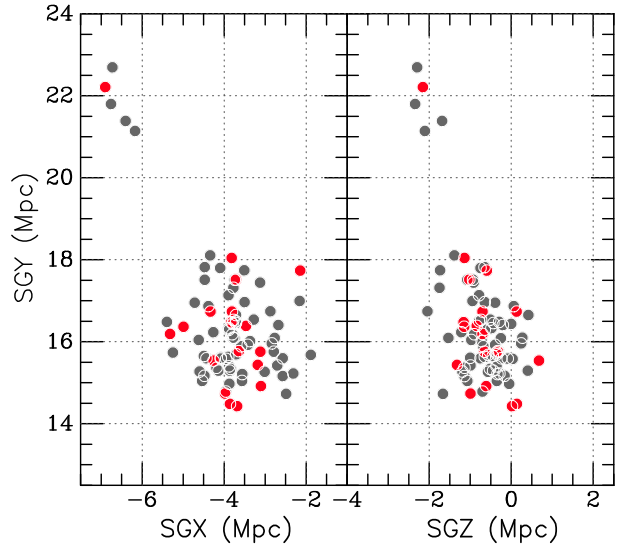


Fig. 1 ACS Virgo SBF distances in supergalactic coordinates. Line-of-sight distance is roughly along the supergalactic y axis (SGY). The most luminous galaxies (a complete magnitude-limited subsample) are shown in red. The 5 galaxies near $SGY \approx 22$ Mpc are projected within the Virgo cluster on the sky, but are members of a background group centered on the giant elliptical NGC 4365.

in Mei et al. (2005a), the problem was solved using a damped sinc function for the interpolation kernel. The calibration was also a challenge. The large range in galaxy luminosity (a factor of over 400) was attended by a large range in color, and with the high precision of the ACS measurements, the usual linear calibration (Tonry et al. 1997, 2001; Blakeslee et al. 2001; Jensen et al. 2003; Mieske et al. 2006) proved inadequate (Mei et al. 2005b). Once these issues were addressed, the quality of the results were unprecedented, with a mean distance modulus error of 0.07 mag, or about 0.5 Mpc for Virgo. This enabled the first clear resolution of the line-of-sight depth of Virgo, as reported by Mei et al. (2007).

Figure 1 shows the ACSVCS SBF distances in supergalactic coordinates. The most obvious feature is the group of 5 galaxies, the brightest being NGC 4365, about 6 Mpc beyond the main concentration of Virgo. These galaxies are within the Virgo cluster on the sky, and even have the same mean radial velocity as a result of their infall motion from the far side. However, the SBF distances clearly reveal them as a distinct group. The cluster itself has a triaxial structure with axial ratios 1:0.7:0.5, with the smallest extent being in the supergalactic z direction. The total line-of-sight depth is approximately 2.4 Mpc (based on a 0.6 Mpc rms depth). In addition to the NGC 4365 group, another grouping of galaxies associated with NGC 4406 (M86) is about 1 Mpc beyond the mean cluster distance and

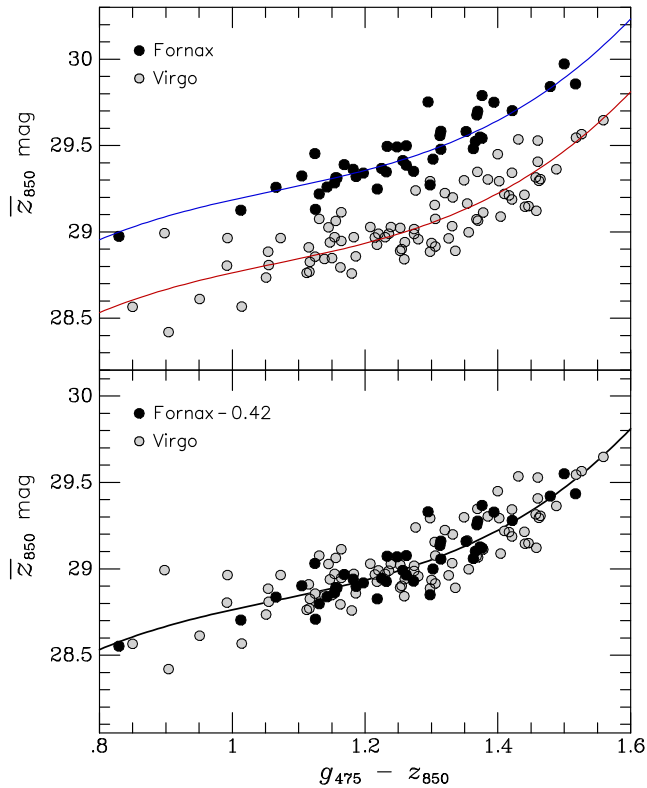


Fig. 2 SBF \bar{z}_{850} magnitude versus $(g_{475}-z_{850})$ color for the combined ACS Virgo and Fornax samples. The curves show the best-fit cubic polynomial for the full sample of galaxies, assuming the value of the relative Fornax-Virgo distance modulus $\Delta(m-M)_{FV}$ that gave the minimum χ^2 . The lower panel shows the two samples shifted together by subtracting the best-fit $\Delta(m-M)_{FV} = 0.42 \pm 0.02$ mag from the Fornax galaxy SBF magnitudes.

has a high (negative) velocity through the cluster. The two most luminous galaxies, M87 and M49, both have distances consistent with the cluster mean; the spatial distribution of dwarf galaxies is very similar to that of the giants. For additional results on Virgo structure, see Mei et al. (2007). Recalibrated distances for the sample galaxies are given in Blakeslee et al. (2009).

2.2 ACS Fornax Cluster Survey

The ACS Fornax Cluster Survey (ACSFCS, Jordán et al. 2007) targeted a complete sample of 43 early-type galaxies in Fornax, the next nearest cluster after Virgo. The goals and observing strategy were very similar to those of the ACSVCS. The compact structure of Fornax makes it useful for distance calibrations. Consequently, one of the primary goals of the ACSFCS was to refine the ACS z_{850} -band SBF calibration, in addition to deriving the relative distance between the Virgo and Fornax clusters. An accurate relative distance is essen-

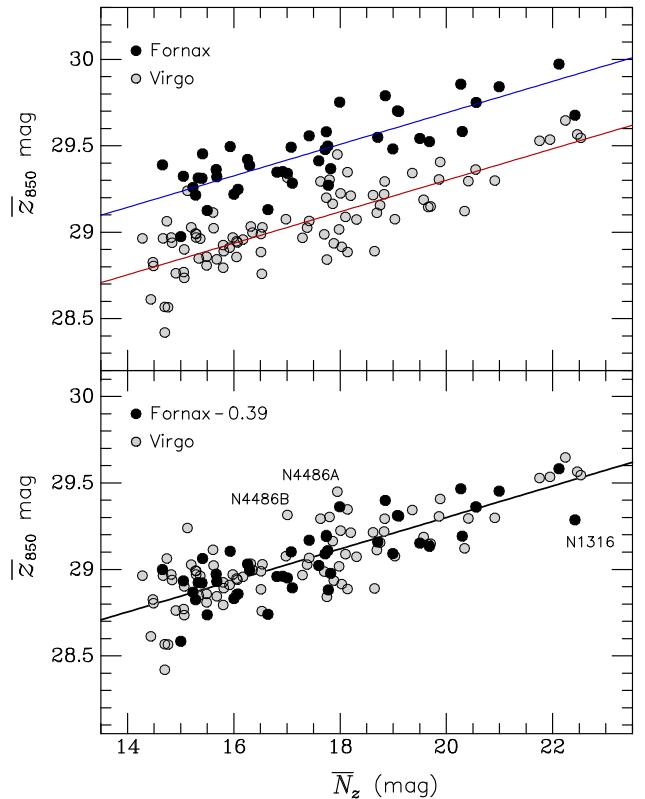


Fig. 3 SBF calibration similar to Figure 2, but based on the z_{850} -band “fluctuation count” \bar{N}_z . A linear fit works well, but the scatter is larger than for the polynomial calibration against $(g_{475}-z_{850})$. The best-fit relative distance modulus $\Delta(m-M)_{FV} = 0.39 \pm 0.03$ mag is consistent with that from the color calibration, despite the potential for environmental bias in this relation with \bar{N} (see text). The luminous blue post-merger Fornax galaxy NGC 1316 is a prominent outlier at the bright end because its SBF magnitude is “too bright” for its luminosity, while under-luminous red galaxies such as the tidally stripped companions of NGC 4486 (M87) scatter above the mean relation because their SBF is relatively “too faint.” The calibration of SBF against color is immune to such effects.

tial for making useful comparisons between these two fiducial clusters.

Figure 2 shows the measured ACS z_{850} SBF magnitudes as a function of $(g_{475}-z_{850})$ colors for both the Virgo and Fornax samples (Blakeslee et al. 2009). The curves show the cubic polynomial calibration fitted to the combined sample (omitting the five ACSVCS galaxies in the background group). The offset in magnitudes was varied, and the minimum χ^2 occurs for a relative Fornax-Virgo distance modulus of $\Delta(m-M)_{FV} = 0.42 \pm 0.02$ mag. Thus, the Fornax cluster is 21% more distant than Virgo, or at 20 Mpc for the adopted distance zero point. Although this relative distance is consistent with some previous studies, the precision here is far higher. The intrinsic scatter in the SBF versus color

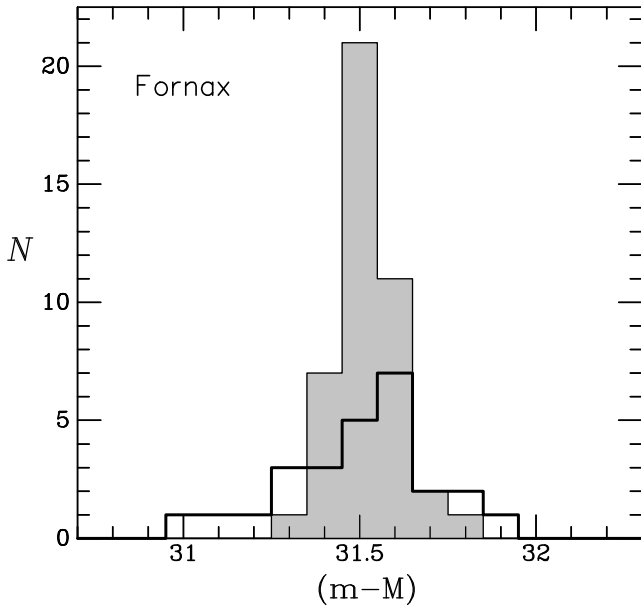


Fig. 4 Comparison of Fornax galaxy ACS SBF distance moduli from Blakeslee et al. (2009, gray-filled histogram) with Fornax ground-based SBF distances from Tonry et al. (2001, thick-lined open histogram). SBF measurements are possible for many more galaxies using *HST*/ACS, and the resulting distance distribution is much tighter than in the earlier ground-based data (for which the histogram width mainly reflects measurement error).

relation is only 0.06 mag for the galaxies in this sample with $(g_{475} - z_{850}) > 1$. The calibration “flares out” at bluer colors, although this is mainly evident for the Virgo sample and could be partly the result of distance variations. Unlike the situation for Virgo, there is no evidence for significant substructure in the Fornax cluster from the ACSFCS sample.

Blakeslee et al. (2009) also presented an alternative SBF calibration based on the ‘fluctuation count’ parameter $\overline{N} = \overline{m} - m_{\text{tot}}$, first introduced by Tonry et al. (2001) and tested for calibration of the ground-based data by Blakeslee et al. (2002), where m_{tot} is the total apparent galaxy magnitude. \overline{N} corresponds to the luminosity of the galaxy in units of the luminosity-weighted mean stellar luminosity. It is therefore a distance-independent measure of the galaxy mass and correlates with \overline{m} as a result of the galaxy mass-color relation. Figure 3 shows the calibration based on \overline{N} , which is approximately linear and yields a consistent relative distance (within the uncertainties) but with a larger intrinsic scatter of ~ 0.10 mag.

Unlike the calibration based on color, which is based purely on stellar population properties, the relation with \overline{N} involves scaling relations similar to the fundamental plane. Thus, luminous blue galaxies, which may have experienced recent star formation and there-

fore have SBF magnitudes “too bright” for their large luminosities, and small red galaxies, which may be tidally stripped and therefore have SBF magnitudes “too faint” for their luminosities, will deviate from the mean relation. Moreover, the \overline{N} relation is likely to have an environmental dependence. For example, if the galaxies in Fornax are younger on average than those in Virgo, the distance offset from the \overline{N} calibration would be underestimated. For these reasons, the calibration based on color is preferable, but \overline{N} provides an alternative when an appropriate color is unavailable. For example, Cantiello et al. (2011) have used a calibration based on \overline{N} to derive distances for 12 galaxies observed with the VLT. Moreover, \overline{N} is an interesting quantity in its own right, and can be used to construct distance-independent color-magnitude diagrams.

2.3 An Improved *I*-band Calibration and Comparisons to Ground-based SBF Distances

Figure 4 shows a comparison of the color-calibrated ACSFCS SBF distances from Blakeslee et al. (2009) to the ground-based Fornax SBF distances from Tonry et al. (2001). The two surveys agree well in the mean, but the distribution of distance moduli has an rms dispersion of 0.092 mag for the ACS data, compared to 0.21 mag for the ground-based SBF data. These dispersions include contributions from intrinsic scatter (~ 0.06 mag) and the depth of Fornax (~ 0.05 mag, estimated from the distribution on the sky), which are the same for the ACS and ground-based data. Thus, the actual measurement errors are about 4 times smaller for the ACS data. The reasons for this vast improvement include a much stronger signal due to the sharper PSF, the ability to identify and remove contaminants to much fainter levels, the improved stability of the PSF, and the photometric homogeneity of the ACS data. The ACS/WFC on *HST* is an almost ideal instrument for optical SBF measurements, although a still larger field would allow better sky estimation for large galaxies.

The ACS Virgo and Fornax surveys used the z_{850} bandpass for SBF measurements, as noted above. Although this provided excellent distances with only one orbit per galaxy, z_{850} is not the most efficient filter. The F814W bandpass (I_{814}) is similar to the Cousins *I*-band used for the ground-based SBF survey (Tonry et al. 1997, 2001) and has a throughput more than twice that of z_{850} , making I_{814} preferable for SBF studies of more distant galaxies that would require multi-orbit observations. Although there had been some I_{814} SBF studies that used a transformed version of the ground-based calibration (Cantiello et al.

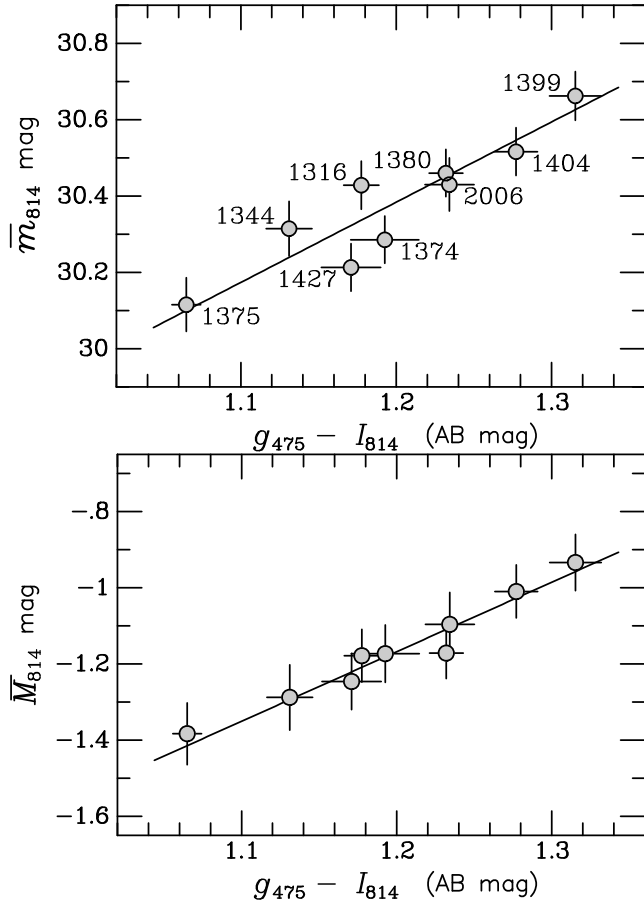


Fig. 5 The F814W SBF calibration. The top panel shows the measured apparent SBF magnitudes as a function of $(g_{475} - I_{814})$ color for nine Fornax galaxies, labeled by their NGC or IC numbers. The lower panel shows absolute SBF magnitudes using the z_{850} SBF distance moduli from the ACSFCS. The lines indicate linear fits, with the coefficients reported by Blakeslee et al. (2010). The very small scatter in the lower panel results from the intrinsic correlation between SBF measurements in the very similar I_{814} and z_{850} bandpasses.

2007a,b; DeGraaff et al. 2007) or a theoretical calibration (Biscardi et al. 2008), an empirical calibration for the ACS I_{814} band was needed for improved reliability.

Figure 5 presents the empirical I_{814} SBF calibration based on 9 bright early-type galaxies in the Fornax cluster (Blakeslee et al. 2010). The top panel shows the relation between apparent SBF magnitude and $(g_{475} - I_{814})$ color; the scatter is 0.06 mag. When the measured z_{850} SBF distances from the ACSFCS are used to derive absolute I_{814} SBF magnitudes, the resulting relation shown in the lower panel has a scatter of only 0.03 mag. This small scatter, which is less than expected from stellar population variations at a given color, results because the intrinsic scatter in the SBF magnitudes is correlated for the very similar I_{814} and

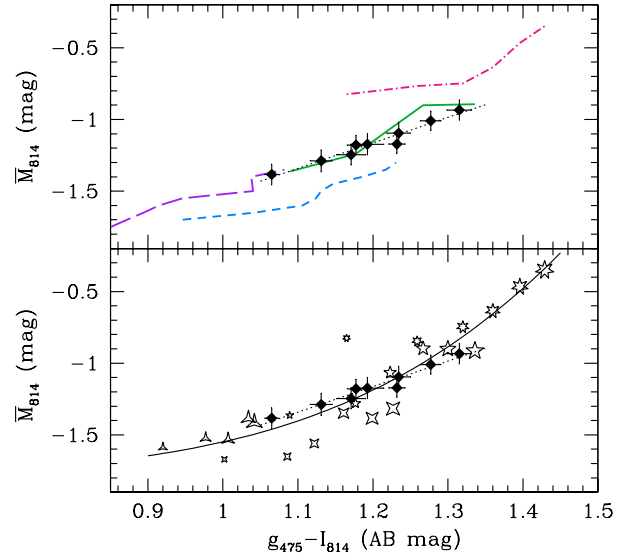


Fig. 6 Calibrating SBF as a primary distance indicator. The top panel shows predicted curves for Teramo/SPoT models with metallicities $[\text{Fe}/\text{H}] = -0.7, -0.3, 0.0, +0.3$ (long-dashed purple, short-dashed blue, solid green, and dot-dashed red curves, respectively) and ages from 3 to 14 Gyr. The solar metallicity model predictions follow the data points (black diamonds) and empirical linear relation (dotted line), without adjustment in zero point. The bottom panel is similar to the top, but here the individual models are represented by discrete points, with different symbols for different metallicities, and symbol size increasing with age. The curve is a cubic polynomial fit to the plotted models; within the color range of the data points, the relation is fairly linear, but the models predict increased curvature beyond this range, similar to what has been observed for the z_{850} -band over a larger empirical color range.

z_{850} bands. This helps to ensure consistency in the distances derived from data in these two bands; see the original work for further discussion. A linear fit to the calibration in Figure 5 suffices because the galaxies are all relatively red, and the curvature is only expected to become significant at bluer colors.

A major part of this ACS I_{814} SBF calibration study included further comparisons between the ground-based SBF distances from Tonry et al. (2001) and the *HST*/ACS SBF distances. The results are given in Appendix A of Blakeslee et al. (2010), which includes a correction formula, based on the Tonry et al. (2001) “quality” index Q , for removing a small apparent bias in the ground-based SBF distance compilation. In addition, an offset is derived to bring the Jensen et al. (2003) NICMOS SBF distances into consistency with the ACS and corrected ground-based distances. The interested reader should refer to that Appendix for a detailed discussion of this important issue.

3 SBF as a Primary Distance Indicator

Because the absolute SBF magnitude in a given bandpass is an intrinsic property of a stellar population, it is possible to calibrate the SBF method from theoretical modeling, and there are many examples in the literature (Tonry et al. 1990; Worthey 1993; Liu et al. 2000; Blakeslee et al. 2001; Cantiello et al. 2003; Marín-Franch & Aparicio 2006; Biscardi et al. 2008; González-Lópezlira et al. 2010). Calibrations based on simple stellar population models are complicated when the effects of age and metallicity are not fully degenerate, since it is often unclear which mix of models best match real galaxies. In particular, this makes any theoretical estimation of the intrinsic scatter very difficult. However, model comparisons are useful as a sanity check, at the very least. Mei et al. (2005b) showed that their empirical *HST*/ACS z_{850} SBF calibration agreed reasonably well with the predictions from the Bruzual & Charlot (2003) models, although with a zero-point offset of ~ 0.15 mag. It would be interesting to update this comparison with the newer version of these models that is now available.

Figure 6, from Blakeslee et al. (2010), compares the *HST*/ACS I_{814} SBF data and empirical calibration to the predictions from the Teramo SPoT models (Raimondo et al. 2005; Raimondo 2009), as reported by Biscardi et al. (2008), but transformed to the AB system. The linear empirical calibration matches remarkably well with the predictions from the SPoT solar metallicity models, without any adjustment in the empirical or model zero points. The fitted relations to data and models intersect near the mean color of $(g_{475} - I_{814}) = 1.2$. As the empirical SBF zero point here is tied to Cepheids (Mei et al. 2007; Blakeslee et al. 2010), the consistency with the stellar population model predictions can be taken as an affirmation of the empirical distance scale, which locates the Virgo and Fornax clusters at 16.5 and 20.0 Mpc, respectively. Thus, using SBF as a primary distance indicator, with model calibration given by the polynomial fit in the lower panel of Figure 6, agrees very well with the standard SBF secondary distance indicator.

An example of the use of SBF as a primary distance indicator is given by Biscardi et al. (2008), who measured SBF distances for 4 galaxies with radial velocities in the 4000 to 8000 km s^{-1} range, and thus distances extending beyond 100 Mpc. These authors used a theoretical calibration based on the Teramo SPoT models, and obtained a value for the Hubble constant $H_0 = 76 \pm 6 \text{ km s}^{-1} \text{ Mpc}^{-1}$, where the error bar here reflects the statistical uncertainty. The systematic uncertainty due to the model zero point is harder to quantify, but the

agreement with the best current values for H_0 based on the empirical distance ladder (Freedman & Madore 2010; Riess et al. 2011) is highly encouraging.

4 SBF with WFC3/IR

Although the recent work on SBF in the optical from the ACS and VLT is extremely impressive when compared to earlier ground-based and pre-ACS *HST* studies, perhaps the most exciting prospects for future SBF work lies at near-IR wavelengths. Such statements as this have been commonplace for well over a decade (e.g., Blakeslee et al. 1999), but now, with the installation of the Wide Field Camera 3, with its IR channel (WFC3/IR), on *HST*, the payoff finally appears imminent. The SBF signal is typically an order of magnitude brighter in the near-IR than in the optical, and the characteristics of WFC3/IR make it far more efficient for SBF work than previously available near-IR cameras. A current *HST* program is carrying out a calibration of the SBF method for the F110W and F160W bandpasses of WFC3/IR using observations of 16 Virgo and Fornax cluster galaxies that already have good ACS SBF distance measurements. The new data appear spectacular, with some results on globular clusters from this program presented by Blakeslee et al. (2011). The WFC3/IR F160W image of the Virgo galaxy IC 3032 is shown in Figure 7, before and after galaxy model subtraction. The fluctuation signal is extremely high.

The combination of the bright near-IR SBF signal with the high throughput and wide field of WFC3/IR should make it possible to obtain an accurate SBF distance whenever an early-type, or bulge-dominated, galaxy is observed in the calibrated passbands at distances reaching beyond 150 Mpc, well out into the Hubble flow. Eventually, once a large number of galaxies have been observed across the sky with WFC3/IR, SBF measurements from archival data could enable highly detailed mapping of the mass density distribution in the local universe. However, some aspects of the WFC3/IR SBF analysis require further testing, and the intrinsic scatter in the SBF calibration at these near-IR wavelengths still needs to be quantified with the same precision as for the ACS F814W and F850LP bandpasses. The results from this effort are expected in the near future!

5 Summary

The SBF method has been in use for over two decades. The survey of 300 galaxy distances published by

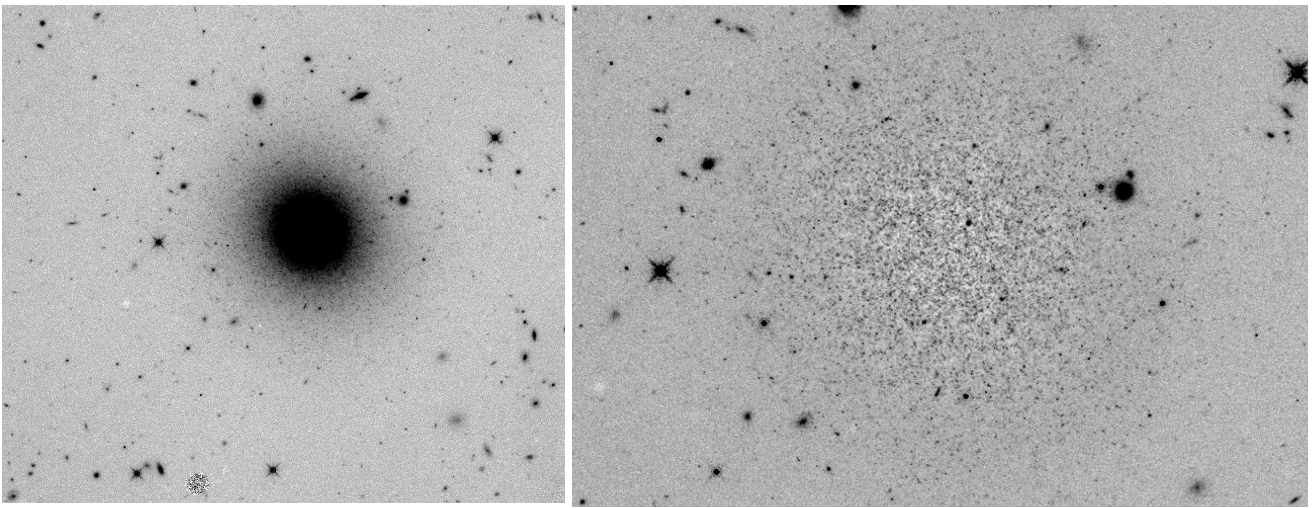


Fig. 7 WFC3/IR image of the Virgo galaxy IC 3032 in the F160W bandpass (left); an enlarged view of the image after galaxy model subtraction (right). The fluctuations are evident.

Tonry et al. (2001) has proven to be a valuable resource for numerous different studies requiring large numbers of nearby galaxy distances. However, the reliability and precision of that survey was limited by the heterogeneous, and sometimes barely adequate, quality of those 1990s-era ground-based data. During the same period, some SBF efforts were made with WFPC2 on *HST*, but that instrument was far from ideal for SBF measurements. However, the installation of the ACS on *HST* ushered in a renaissance for optical SBF studies. To date, *HST*/ACS SBF distances have been published for 136 galaxies in the directions of the Virgo and Fornax clusters, compared to fewer than 60 in the ground-based SBF survey. The distance errors (including intrinsic stellar population scatter in the method, but omitting systematic zero-point uncertainty) for the ACS SBF measurements are typically 4-5%, as compared to 10% or more for the ground-based SBF measurements. The measurement errors (omitting intrinsic scatter) are several times smaller for the ACS samples, and this has allowed quantification of the quality-related bias in the ground-based SBF distances.

We now have an excellent calibration for the SBF method in the F814W and F850LP bandpasses of ACS, and this has allowed us to probe the internal structure of the Virgo cluster and measure the Fornax/Virgo distance ratio with unprecedented precision. Recent stellar population models support the empirically based distance zero point and allow SBF to be applied with confidence as a primary distance indicator. With the proper calibration and control of systematics, the space-based SBF method is the most accurate way of measuring the distances to early-type galaxies in the important ~ 10 to ~ 100 Mpc distance range. It is straightfor-

ward at smaller distances, but resolved stellar population methods are then competitive, and at larger distances the peculiar velocities are generally a small fraction of the Hubble velocity. This leaves a large volume for SBF studies. Additional data are in hand and efforts are ongoing to bring the Coma cluster into the tight ACS SBF distance ladder and to probe structures at even larger distances.

The installation of the WFC3 instrument with its IR channel on *HST* promises to engender a similar renaissance for the near-IR SBF method as ACS did for optical SBF. In fact, the relative advance will likely be even greater, given the vastly lower sky background for near-IR observations from space. We have shown the high quality of the WFC3/IR data. Our efforts now are focused on producing an SBF calibration for WFC3/IR comparable to that obtained for ACS and characterizing the internal scatter in the method at these wavelengths. Given the very modest exposure times required for near-IR SBF measurements, the availability of such a calibration will greatly improve the potential for distance and velocity studies from the large cache of *HST* imaging data. Much work remains to be done in this area: as the saying goes, “The harvest is plentiful, but the workers are few.” The best is yet to come.

Acknowledgements I am indebted to my sundry SBF collaborators, including my colleagues from the ACS Virgo and Fornax cluster surveys, for their many contributions to the work described here. This paper is based on an invited review talk at the conference, “Fundamental Cosmic Distance Scale: State of the Art and the Gaia Perspective.” I thank the conference organizers for an excellent meeting and for inviting me to talk on this subject.

References

- Ajhar, E. A., Tonry, J. L., Blakeslee, J. P., Riess, A. G., & Schmidt, B. P. 2001, *Astrophys. J.*, 559, 584
- Barber DeGraaff, R., Blakeslee, J. P., Meurer, G. R., & Putman, M. E. 2007, *Astrophys. J.*, 671, 1624
- Biscardi, I., Raimondo, G., Cantiello, M., & Brocato, E. 2008, *Astrophys. J.*, 678, 168
- Blakeslee, J. P. 2009, *American Institute of Physics Conference Series*, 1111, 27
- Blakeslee, J. P., Ajhar, E. A., & Tonry, J. L. 1999, *Post-Hipparcos Cosmic Candles*, 237, 181
- Blakeslee, J. P., Cantiello, M., Mei, S., et al. 2010, *Astrophys. J.*, 724, 657
- Blakeslee, J. P., Cho, H., Peng, E. W., et al. 2012, *Astrophys. J.*, 746, 88
- Blakeslee, J. P., Jordán, A., Mei, S., et al. 2009, *Astrophys. J.*, 694, 556
- Blakeslee, J. P., Lucey, J. R., Tonry, J. L., et al. 2002, *Mon. Not. R. Astron. Soc.*, 330, 443
- Blakeslee, J. P., Vazdekis, A., & Ajhar, E. A. 2001, *Mon. Not. R. Astron. Soc.*, 320, 193
- Bruzual, G. & Charlot, S. 2003, *Mon. Not. R. Astron. Soc.*, 344, 1000
- Cantiello, M., Raimondo, G., Brocato, E., & Capaccioli, M. 2003, *Astron. J.*, 125, 2783
- Cantiello, M., Blakeslee, J. P., Raimondo, G., et al. 2005, *Astrophys. J.*, 634, 239
- Cantiello, M., Blakeslee, J., Raimondo, G., Brocato, E., & Capaccioli, M. 2007a, *Astrophys. J.*, 668, 130
- Cantiello, M., Raimondo, G., Blakeslee, J. P., Brocato, E., & Capaccioli, M. 2007b, *Astrophys. J.*, 662, 940
- Cantiello, M., Brocato, E., & Capaccioli, M. 2011, *Astron. Astrophys.*, 534, A35
- Ciardullo, R., Feldmeier, J. J., Jacoby, G. H., et al. 2002, *Astrophys. J.*, 577, 31
- Côté, P., Blakeslee, J. P., Ferrarese, L., et al. 2004, *Astrophys. J. Suppl. Ser.*, 153, 223
- Ferrarese, L., et al. 2000, *Astrophys. J.*, 529, 745
- Freedman, W. L. & Madore, B. F. 2010, *Annu. Rev. Astron. Astrophys.*, 48, 673
- González-Lópezlira, R. A., Bruzual-A., G., Charlot, S., Ballesteros-Paredes, J., & Loinard, L. 2010, *Mon. Not. R. Astron. Soc.*, 403, 1213
- Lee, H.-c., Worthey, G., & Blakeslee, J. P. 2010, *Astrophys. J.*, 710, 421
- Liu, M. C., Charlot, S., & Graham, J. R. 2000, *Astrophys. J.*, 543, 644
- Jensen, J. B., Tonry, J. L., & Luppino, G. A. 1998, *Astrophys. J.*, 505, 111
- Jensen, J. B., Tonry, J. L., Barris, B. J., et al. 2003, *Astrophys. J.*, 583, 712
- Jordán, A., Blakeslee, J. P., Côté, P., et al. 2007, *Astrophys. J. Suppl. Ser.*, 169, 213
- Marín-Franch, A. & Aparicio, A. 2006, *Astron. Astrophys.*, 450, 979
- Mei, S., Blakeslee, J.P., Tonry, J.L., et al. 2005a, *Astrophys. J. Suppl. Ser.*, 156, 113
- Mei, S., Blakeslee, J.P., Tonry, J.L., et al. 2005b, *Astrophys. J.*, 625, 121
- Mei, S., Blakeslee, J. P., Côté, P., et al. 2007, *Astrophys. J.*, 655, 144
- Mieske, S., Hilker, M., & Infante, L. 2006, *Astron. Astrophys.*, 458, 1013
- Mould, J., & Sakai, S. 2009, *Astrophys. J.*, 694, 1331
- Raimondo, G. 2009, *Astrophys. J.*, 700, 1247
- Raimondo, G., Brocato, E., Cantiello, M., & Capaccioli, M. 2005, *Astron. J.*, 130, 2625
- Riess, A. G., Macri, L., Casertano, S., et al. 2011, *Astrophys. J.*, 730, 119
- Tonry, J.L., Ajhar, E.A., & Luppino, G.A. 1990, *Astron. J.*, 100, 1416
- Tonry, J. L., Blakeslee, J. P., Ajhar, E. A., & Dressler, A., 1997, *Astrophys. J.*, 475, 399
- Tonry, J. L., Blakeslee, J. P., Ajhar, E. A., & Dressler, A., 2000, *Astrophys. J.*, 530, 625
- Tonry, J.L., Dressler, A., Blakeslee, J.P., et al. 2001, *Astrophys. J.*, 546, 681
- Tonry, J.L. & Schneider, D.P. 1988, *Astron. J.*, 96, 807
- Worthey, G. 1993, *Astrophys. J.*, 409, 530